



PERFORMANCE ANALYSIS & COMPARISON OF VSC-BASED SHUNT AND SERIES COMPENSATORS FOR LOAD VOLTAGE CONTROL IN DISTRIBUTION SYSTEMS

M.Padmarasan¹, C.T.Manikandan²,
K.P.Nithya³, R.Subbulakshmy⁴

^{1,2,3,4}Assistant Professor, Department of EEE, Panimalar Institute of Technology, Chennai, (India)

ABSTRACT—In this paper, the performance of voltage source converter-based shunt and series compensators used for load voltage control in electrical power distribution systems has been analyzed and compared, when a nonlinear load is connected across the load bus. The comparison has been made based on the closed loop frequency response characteristics of the compensated distribution system. A distribution static compensator (DSTATCOM) as a shunt device and a dynamic voltage restorer (DVR) as a series device are considered in the voltage control mode for the comparison. The power quality problems which these compensator address include voltage sags/swells, load voltage harmonic distortions, and unbalancing. The effect of various system parameters on the control performance of the compensator can be studied using the proposed analysis. In particular, the performance of the two compensators is compared with the strong ac supply (stiff source) and weak ac-supply (non-stiff source) distribution system. The experimental verification of the analytical results derived has been obtained using a laboratory model of the single-phase DSTATCOM and DVR. A generalized converter topology using a cascaded multilevel inverter has been proposed for the medium-voltage distribution system. Simulation studies have been performed in the PSCAD/EMTDC software to verify the results in the three-phase system.

Keywords—Distribution Static Compensator (DSTATCOM), Dynamic Voltage Restorer (DVR), Frequency Response Characteristic, Load Voltage Control, Multilevel Inverter, Nonlinear Load.

I INTRODUCTION

The voltage related power-quality (PQ) problems, such as sags and swells, voltage dips, harmonic distortions due to nonlinear loads and voltage unbalancing in electrical power distribution systems, have been a major concern for the voltage sensitive loads [1]. Load voltage regulation using VSC for different grid



connected applications has been recently attempted in [2]–[4]. With the increased use of power-electronics devices in the consumer products, the loads are becoming voltage sensitive and nonlinear in nature. Depending upon the applications, these loads are connected to the distribution system having varying voltage and power levels. Also the radial feeders of the distribution system to which these loads are connected have varying length and short circuit current (SCC) levels. This depends upon the location of the load, distribution system size, and its voltage and volt-ampere (VA) ratings. This leads to the wide variations in the Thevenin's equivalent feeder impedance looking from the load side. If the load is connected at the end of the long feeder and has small short circuit current value, it is called a weak ac supply system (or non-stiff source) [5]. Similarly, if the load is connected close to the feeder, it is referred to as strong ac supply system (or stiff source). The line impedance of these feeders is very small or negligible.

Two types of VSC-based compensators have been commonly used for mitigation of the voltage sags and swells and regulating the load bus voltage [7], [8]. The first one is a shunt device, which is commonly called DSTATCOM [9]–[12], and the second one is a series device, which is commonly called DVR [13]–[16]. In [10] and [17]–[20], these compensators can address other PQ issues, such as load voltage harmonics, source current harmonics, unbalancing, etc., under steady state to obtain more benefits out of their continuous operation. There have been a variety of control strategies proposed for load voltage control using the aforementioned two devices. For DSTATCOM, this includes reactive power compensation [21] and voltage-control mode operation of DSTATCOM [9]–[11], [17].

For DVR, it includes open-loop and closed-loop load voltage-control methods [22]. The closed-loop voltage-control mode operation of the two devices is considered best from the point of view of precise and fast control against sudden variations in the supply voltage and the load [23]. In [24], a common control strategy has been proposed for the shunt and series compensator.

A detailed study of the dynamic performance of these two compensating devices controlling the load voltage under closed loop is required. This study presumes a three-phase, four-wire distribution system [5], [7], [9]–[11], in which each phase is controlled independently. Under this situation, the result obtained on the per phase basis is equally applicable for the three-phase system.

In this paper, the performance of the DSTATCOM and the DVR used for the load bus voltage control have been analyzed and compared when a nonlinear load is connected across the load bus. Both of these compensators are used under closed-loop voltage-control mode. The control performance of the compensator and attenuation properties against perturbations has been obtained using closed-loop frequency-response characteristics. A simple output voltage feedback control and a fixed switching frequency linear modulation have been used for the operation of the VSC under closed loop. It is shown that the performance of two compensating devices depends upon the feeder impedance. The performance study for the DSTATCOM and the DVR has been obtained for the weak and strong ac supply systems. The experimental verification of the analytical results derived is obtained through the laboratory model of a single-phase distribution system, using field-programmable gate-array (FPGA)-based implementation of the controller and modulation of the VSC. A

generalized converter topology is considered and the modulation technique based on the cascaded multilevel inverter has been proposed for medium-voltage distribution system applications [25]. Simulation studies have been performed to verify the results in a three-phase distribution system.

II VSC-BASED SHUNT AND SERIES COMPENSATORS

The single-phase equivalent of a radial distribution system is shown in Fig. 1. The feeder and load of the distribution are shown in Fig. 1(a) and (b), respectively. The source v_s is considered to be the starting point of the radial feeder. The point of common coupling (PCC), represented by point P, is a particular bus of the feeder to which a nonlinear load is connected. The voltage at the point P is denoted by v_t . The Thevenin's equivalent feeder impedance is represented by inductance L_s and re-sistance R_s . Restoring the load bus voltage v_l at point L under the conditions of sags and swells in the source is an essential re-quirement for the sensitive loads. Also, it is required to control this voltage against distortions due to the nonlinear load [26]. A VSC-based generalized structure of the compensator used in a single-phase distribution system is shown in Fig. 1(c). Two types of compensators have been considered in this paper for load voltage control of the distribution system.

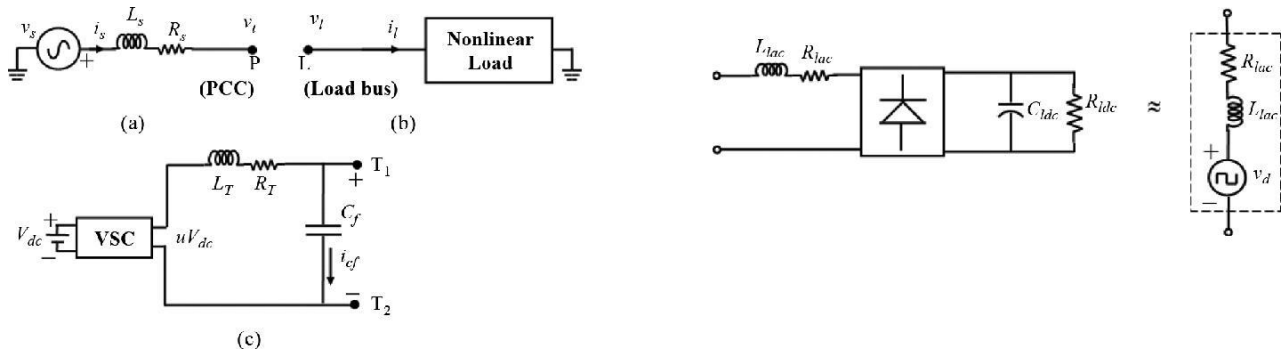


Fig. 1. Compensator structure used for load voltage control for a 1-φ system. (a) Feeder. (b) Load. (c) Compensator.

In case the compensator is shunt type (i.e., DSTATCOM), the terminals P, L, and T1 are joined together and T2 is grounded. In case the compensator is series type (i.e., DVR), the terminal T1 is connected to L and T2 is connected to P. The compensator consists of a VSC that is interfaced to the distribution system.

The voltage V_{dc} represents the net dc link voltage across the VSC. The variable u is defined as the control input and represents the high-frequency switching of the inverter that assumes discrete values between $+1$ and -1 , depending upon the number of levels used in the multilevel converter topology [17], [27]. The symbol L_T represents the equivalent inductance in the converter circuit. The resistance R_T represents the equivalent loss component in the compensator. The filter capacitor C_f is connected across the VSC to support the output voltage and provide filtering to the high-frequency switching components of the VSC. The currents flowing

through the different branches are: the source current i_s , the load current i_l , and the current through the filter capacitor i_{cf} .

The nonlinear load considered in this paper is assumed to be a bridge rectifier type with input impedance ($L_{lac}R_{lac}$) [4]. For a single-phase load as shown in Fig. 2, the output dc voltage of the bridge rectifier is fed to a resistive load R_{ldc} supported by a parallel dc capacitor C_{ldc} . This nonlinear load is called a voltage source type and is represented by a harmonic perturbation voltage source v_d , where v_d is the Thevenin equivalent voltage source of this load [11], [17], [28]. For a large dc capacitor C_{ldc} and ac inductance L_{lac} , the input impedance (R_{lac}) approximately represents the Thevenin equivalent impedance of this nonlinear load. The approximate equivalent of this type of nonlinear load is also shown in Fig. 2.

2.1 DSTATCOM Model

The single-phase equivalent circuit of a DSTATCOM compensated distribution system is shown in Fig. 3. The VSC is used for the injection of the controllable ac voltage uV_{dc} in order to control the load bus voltage v_l under the closed loop. The dc link voltage may be self-supported by a dc-link capacitor for the case of DSTATCOM [10]. The current injected in the shunt path is denoted by i_{sh} . A voltage-source-type nonlinear load as considered in Fig. 2 is connected with the Thevenin equivalent voltage v_d and impedance ($L_{lac}R_{lac}$).

Choosing the state vector $x_T = [i_{sh} \ i_{cf} \ v_l]$ and considering the load voltage v_l as output, the following state space representation can be derived:

$$\begin{aligned} \dot{x} &= Ax + b_1 v_s + b_2 u + b_3 v_d \\ (1) \quad v_l &= cx \end{aligned}$$

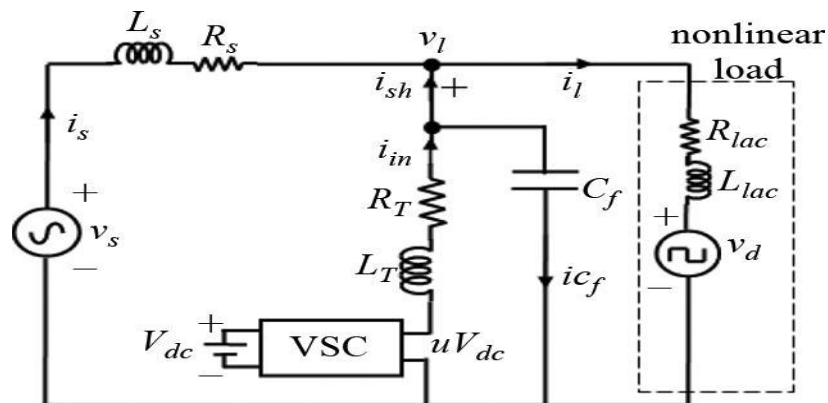


Fig. 3. Equivalent circuit of a DSTATCOM-compensated distribution system

2.2 DVR Model

The single-phase equivalent circuit of a DVR-compensated distribution system is shown in Fig. 4. In the direct control scheme presented in this paper, the DVR injects the controllable ac voltage uV_{dc} in order to control the load bus voltage v_l under closed loop. The dc link voltage in this case may be supported by grid-connected rectifier

[19] or separate energy storage [29]. The current flowing through the VSC is defined as the series current i_{se} . The source current i_s is assumed the same as the load current i_l in this case. The remaining system parameters and variables are the same as defined for the DSTATCOM model in Fig. 3.

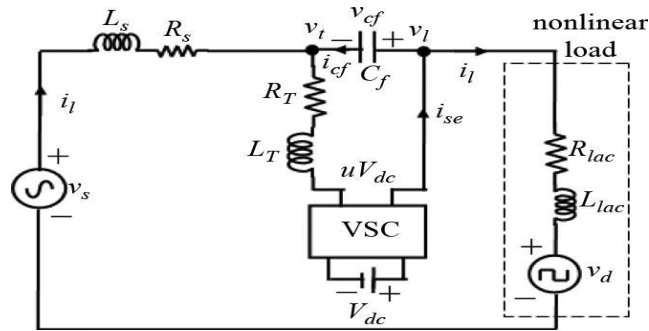


Fig. 4. Equivalent circuit of a DVR-compensated distribution system.

Choosing the state vector $x_T = [v_{cf} \ i_{se} \ i_l]$ and considering the load voltage v_l as output, the following state space representation can be derived:

$$\dot{x} = Ax + b_1 v_s + b_2 u + b_3 v_d$$

$$(2) \quad v_l = R_{lac} i_l + L_{lac} \frac{di_l}{dt} + v_d = cx + qv_s + wv_d$$

III LOAD VOLTAGE CONTROL AND VSC MODULATION

It has been shown for DSTATCOM in [10], [11], [17] and for DVR in [15] that the closed-loop control is achieved using voltage and current feedback loops. In this paper, a simple output voltage feedback control is used for the control of the load bus voltage. In this scheme, the actual load voltage v_l is fed back and compared with the reference voltage v_{lref} . The error e_l so obtained is passed through the proportional plus low-pass filtered derivative controller [30] to produce a switching function s_e . The s -domain representation of the controller transfer function $G_c(s)$ between the output switching function s_e and the input error function e_l is defined as

$$(3) \quad G_c(s) = \frac{s_e(s)}{e_l(s)} = k_1 + \frac{k_2 s}{\alpha k_2 s + 1}$$

where the error function e_l is defined as $e_l = v_{lref} - v_l$. The constants k_1 and k_2 are the proportional and derivative gains, respectively. The derivative action is associated with the first-order low-pass filter to limit the amplification of the high-frequency noise and disturbances. The low-pass filtering action depends upon the filter coefficient α .

The switching function s_e so obtained is modulated following the phase-shifted multicarrier PWM for the cascaded multilevel converter as given in [17]. The equivalent modulation method used with the two-level converter can be implemented as [11]

$$u(t) = +1, \quad \text{for } s_e(t) - v_{tri}(t) > +h \quad (4a)$$

$$u(t) = -1, \quad \text{for } s_e(t) - v_{tri}(t) < -h \quad (4b)$$

where $v_{tri}(t)$ is a triangular carrier of suitable amplitude V_{tri} and frequency f_c . This modulation scheme leads to the VSC operation at the fixed switching frequency f_c , when the amplitude of the carrier is chosen above a certain minimum amplitude $V_{tri\min}$ [11], [17]. A small hysteresis band h is introduced to avoid the multiple crossings at the intersection in (4). The modulation process represents the linear relation between the input s_e and output u on the average basis. The linear gain of the modulator is represented by $k_d=1/V_{tri}$ [17]. The allowable limit of gain $k_d=1/V_{tri\min}$ increases with an increase in switching frequency; therefore, the tracking characteristics improve at a higher switching frequency [17], [31]. The output of the modulator is delayed by the average switching delay (i.e., half the switching period $T_d=1/2f_c$). In case of the multilevel inverter, f_c represents the effective switching frequency [17].

The effect of the high-frequency switching due to modulation is modeled as a first-order lag. Therefore, in steady state, the modulation process is defined by a transfer function $G_d(s)$ that consists of a fixed gain k_d and a delay function $1/(1+T_d s)$ as

$$(5) \quad G_d(s) = \frac{k_d}{(1 + T_d s)}$$

The complete block diagram of the load voltage control using either DSTATCOM or DVR is shown in Fig. 5.

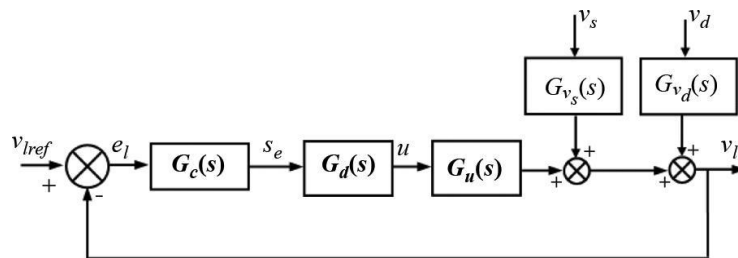


Fig. 5. Block diagram of the load voltage control using DSTATCOM or DVR

The following transfer functions in Fig. 5 can be derived from (1) or (2) for the case of DSTATCOM or DVR, respectively

$$(6) \quad G_u(s) = \left. \frac{v_l(s)}{u(s)} \right|_{v_s=v_d=0} = c(sI - A)^{-1} b_2$$

$$(7) \quad G_{v_s}(s) = \left. \frac{v_l(s)}{v_s(s)} \right|_{u=v_d=0} = c(sI - A)^{-1} b_1 + q$$

$$G_{v_d}(s) = \left. \frac{v_l(s)}{v_d(s)} \right|_{u=v_s=0} = c(sI - A)^{-1} b_1 + q$$



$$(8) \quad G_{vd}(s) = \frac{v_d(s)}{v_d(s)} \Big|_{u=v_s=0} = c(sI - A)^{-1} b_3 + w.$$

Note that the matrices q and w in (7) and (8), respectively, are null matrices for the case of DSTATCOM.

IV TRACKING CHARACTERISTICS USING STEADY-STATE FREQUENCY-RESPONSE ANALYSIS

In this section, the steady-state tracking behavior of the load voltage control using DSTATCOM and DVR are discussed. Comparisons of the tracking characteristics of the two compensating devices are made with reference to the weak and strong ac supply system.

4.1 Weak AC Supply System

Assume a weak (or non-stiff) ac supply system. Consider the per unit system parameters of such a weak ac supply system given in Table I. *DSTATCOM*: Let us first study the tracking characteristics of load bus voltage control using DSTATCOM. The transfer functions $G_u(s)$, $G_{vs}(s)$, and $G_{vd}(s)$ are determined using (6)–(8), respectively. The state space model of DSTATCOM given in (1) is used for obtaining the transfer functions. Under the ideal tracking condition in (4) (i.e., high gain and zero delay in (5) corresponding to infinite switching frequency, and ideal derivative action in (3), that is, $\alpha=0$), the dominant closed-loop pole will lie close to $\lambda = -(k_1/k_2)$ for the closed-loop system shown in Fig. 5. Therefore, the system dynamics will be governed by the time constant $T = k_2/k_1$. However, with practical switching devices (e.g., insulated-gate bipolar transistors (IGBTs) operating at the finite fixed switching frequency), the modulator dynamics are used in Fig. 5. In this situation, the system will have satisfactory stability properties with $(1/T_d) > (1/T)$ (i.e., pole to the left of zero). Now consider a unity gain modulator (i.e., $k_d=1$), and the delay corresponding to 2 kHz of the effective switching frequency of the inverter (i.e., $T_d = 0.25$ ms).

The value of filter coefficient is chosen as 0.01 in (3) for better filtering of high-frequency noise. Fig. 6 shows the closed-loop frequency response of the output load voltage v_l with respect to the reference voltage v_{lref} for the aforementioned data. A comparison is also made in Fig. 6 when the modulator transfer function has changed, corresponding to the high gain (e.g., $k_d =$

5) and high effective switching frequency (e.g., 3 kHz), with $T_d = 0.1667$ ms in (5). The stability properties further improves based on the condition $(1/T_d) > (1/T)$. The rest of the parameter is considered the same as before. It is clear from the figure that the tracking characteristics for the low-frequency references (e.g., 50 Hz) would be better and bandwidth would be higher (better stability) with the high effective switching frequency and higher gain modulator. Though there is also an increased resonant peak as seen from Fig. 6, however, sufficiently higher bandwidth ensures better transient performance under closed loop. Therefore, it is desirable to use high effective switching frequency with high modulator gain for better tracking characteristics. Here onwards, these higher values would be considered for the theoretical analysis in this paper.

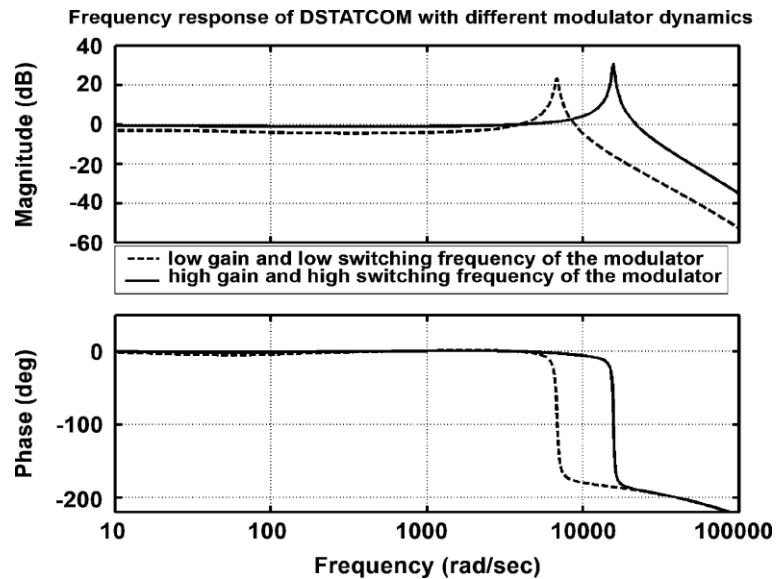


Fig. 6. Comparison of the closed-loop frequency response of DSTATCOM with respect to the reference load voltage v_{ref} for two different modulator dynamics: (first) low gain and low effective switching frequency and (second) high gain and high effective switching frequency, for a weak ac supply system.

Fig. 7 shows the closed-loop frequency response with respect to the source voltage v_s and nonlinear load perturbation voltage v_d . These plots are obtained with respect to the block diagram shown in Fig. 5 and using the transfer functions $G_{vs}(s)$ and $G_{vd}(s)$, obtained from (7) and (8), respectively. The DSTATCOM provides good attenuation with respect to both of these perturbations over a wide range of frequencies. **DVR:** Consider now study of the tracking characteristics of the load bus voltage control using DVR for a weak ac supply system. The transfer functions $G_u(s)$, $G_{vs}(s)$, and $G_{vd}(s)$ for the case of DVR are determined using (6)–(8), respectively. The state space model of DVR given in (2) is used for obtaining these transfer functions. Fig. 8 shows the closed-loop frequency response of the output load voltage v_l with respect to the reference voltage v_{lref} for the same data as considered for the DSTATCOM earlier. The effective switching frequency and gain for the modulator (5) are considered high as for the case of the DSTATCOM. It can be seen from Fig. 8 that the tracking characteristic with the DVR is similar to that of the DSTATCOM shown in Fig. 6. However, the bandwidth of the control loop in case of DVR is reduced considerably compared to that with DSTATCOM.

Fig. 9 shows the closed-loop frequency response with respect to the source voltage v_s and nonlinear perturbation voltage v_d . It is clear from Fig. 9 that with respect to both of these variables, the attenuation decreases at higher frequencies and perturbations pass almost without any attenuation above the bandwidth of the control loop. The DVR can control the load voltage against sags and swells in the source voltage since it provides sufficient attenuation to these low-frequency disturbances in the source voltage. However, as seen in Fig. 9, the presence of high-frequency components in the nonlinear load will appear in the load voltage without any attenuation. Therefore, notches may be present in the load voltage when the load is nonlinear and the feeder is non-stiff, in case of compensation with the DVR.

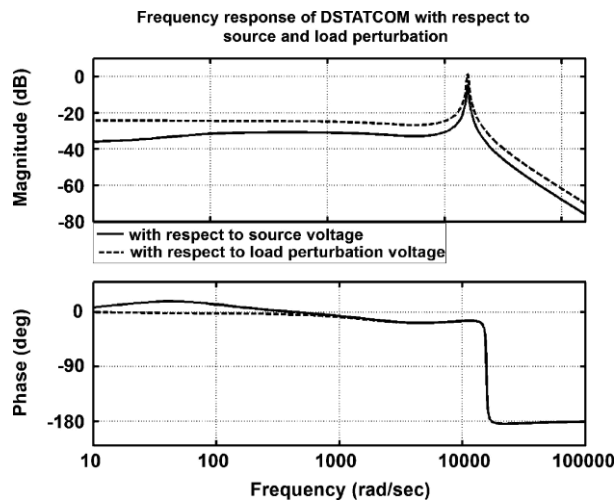


Fig. 7. Closed-loop frequency response of the DSTATCOM with respect to the source voltage v_s and nonlinear load perturbation voltage v_d for a weak ac supply system.

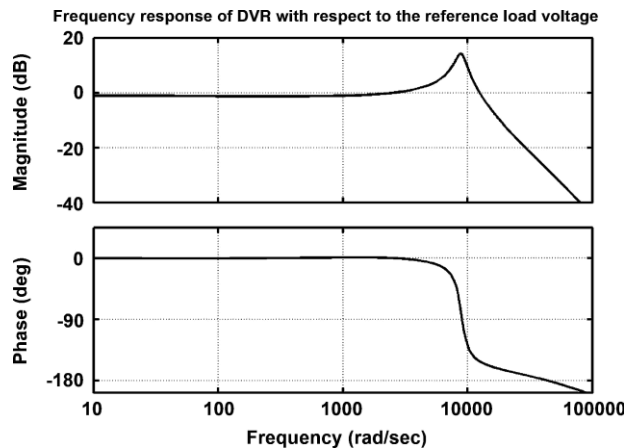


Fig. 8. Closed-loop frequency response of DVR with respect to the reference load voltage v_{ref} for a weak ac supply system.

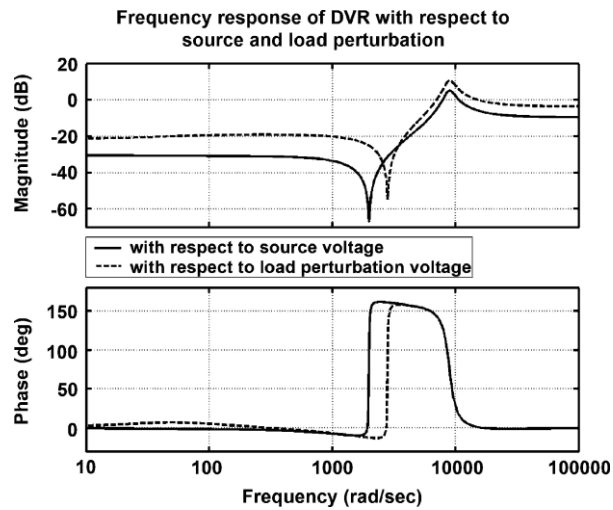


Fig. 9. Closed-loop frequency response of DVR with respect to the source voltage v_s and nonlinear load perturbation voltage v_d for a weak ac supply system.

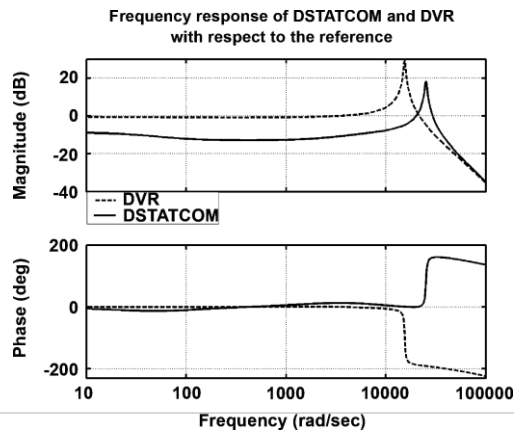




Fig. 10. Comparison of the closed-loop frequency response for DSTATCOM and DVR with respect to the reference load voltage for a strong ac supply system.

4.2 Strong AC Supply System

Assume a strong (or stiff) ac supply system. Consider the same per unit system parameters as given in Table I, except that the per unit feeder impedance is 1/100 or the feeder short-circuit capacity is 100 times that for the case of the weak ac system considered in the previous subsection. Fig. 10 shows the comparison of the closed-loop frequency response of the load voltage control for the DSTATCOM and the DVR, with respect to the reference load voltage. It is clear from the figure that for the case of stiff source, the DSTATCOM has inferior tracking properties and, therefore, cannot control the load voltage, whereas the DVR is effective for the load voltage control in this case. Fig. 11 shows the comparison of the closed-loop frequency response for the DSTATCOM and the DVR with respect to the source voltage and nonlinear load perturbation voltage. It is seen from the figure that attenuation for the DSTATCOM with respect to the source voltage is negligible and, therefore, it is ineffective for sags and swells compensation in this case. The DVR has good attenuation against source voltage and nonlinear load perturbation voltage. Therefore, the DVR is the better option for the load voltage control application in case of the stiff source.

For DSTATCOM, the tracking characteristic largely depends upon the net feeder impedance and it deteriorates at low impedance (strong ac supply system). In particular, low feeder reactance deteriorates attenuation to the harmonic components in source voltage and low feeder resistance deteriorates the capability of DSTATCOM to control the load voltage against sags and swells. For DVR, the tracking characteristic deteriorates at high feeder impedance (weak ac supply system). In this case, high feeder resistance deteriorates load voltage regulation capability of the DVR and high feeder reactance deteriorates compensation against high-frequency components of the nonlinear load.

V EXPERIMENTAL RESULTS

A single-phase experimental model developed in the laboratory has been used to obtain the verification of the analytical results presented in the previous section. The controller and modulation technique used in this paper is implemented in a National Instrument (NI), PXI-7831 reconfigurable input/output (RIO), field-programmable gate array (FPGA), through Lab-VIEW software-based graphical programming. The programs are downloaded on a PXI 8186, remote embedded controller. In addition, the FPGA is also programmed to generate the sinusoidal reference for the load voltage, the frequency of which is synchronized with the supply using a software-based phase-locked loop (PLL). The VSC is implemented using the Mitsubishi, Intelligent Power Module (IPM) PM50CSD120. The load voltage is fed back using LEM, voltage transducer LV 25-P.

The parameters used for the experimental model are given in Table II. In case of the stiff feeder, the ac source is directly connected to the PCC. The controller used is given by (3) with the same parameters as given in Section

IV. The two-level fixed switching frequency closed-loop modulation (4) is used for the operation of the VSC.

The results obtained for the case of weak and strong ac supply systems are discussed as follows.

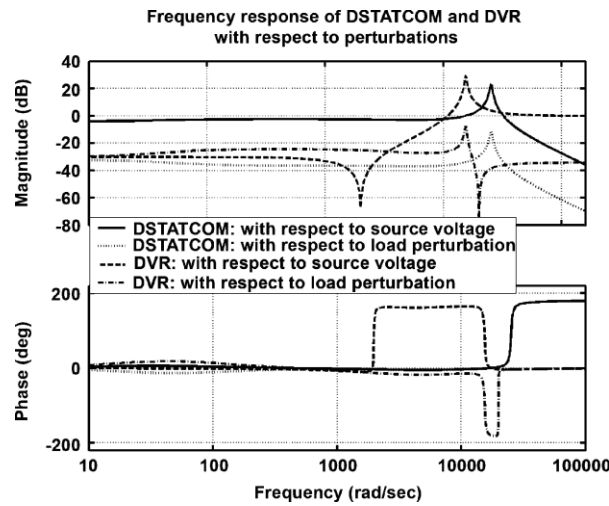
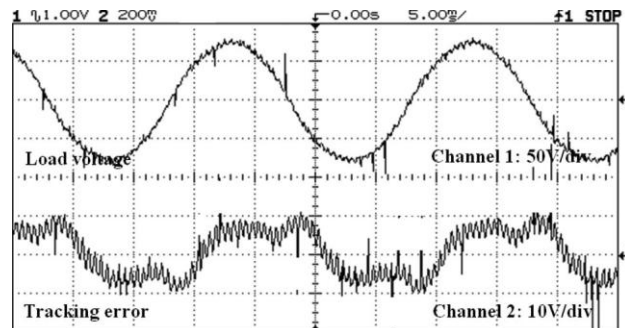


Fig. 11. Comparison of closed-loop frequency response for DSTATCOM and DVR with respect to the source voltage and nonlinear load perturbation for a strong ac supply system.



(a)

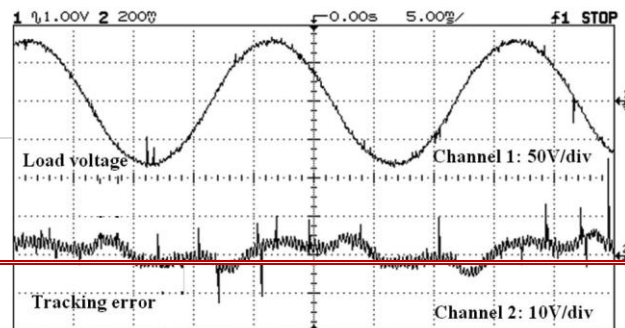


Fig. 12. Comparison of load voltage control using DSTATCOM for the non-stiff supply system, showing load voltage and tracking error (a) at the 2-kHz switching frequency and (b) at the 3-kHz switching frequency.

5.1 Load Voltage Control in a Weak AC Supply System

As discussed earlier, a weak ac system is realized considering the finite impedance in the feeder as given in Table II. First, it is shown that the use of high switching frequency and high gain modulator gives better tracking characteristics as discussed in Section IV-A. With the carrier-based fixed switching frequency closed-loop modulation, the choice of high switching frequency leads to the lower amplitude of the carrier [11] and, hence, high modulator gain [17]. A sinusoidal reference of 60 V(rms) is chosen for the load voltage control. Fig. 12 shows the comparison of the load voltage control using DSTATCOM with 2 kHz and 3 kHz of switching frequency using a two-level VSC. Clearly the voltage tracking characteristic is better with 3-kHz switching frequency showing small tracking error at steady state. Therefore, for the remainder of this paper, the experimental results are shown at the fixed switching frequency of 3 kHz.

In the absence of any compensation and with the distorted source voltage as shown in Fig. 14 and having a total harmonic distortion (THD) of 5.2%, the load voltage gets distorted and has a THD of 21.8% and a magnitude reduced by 10%, due to the nonlinear load and distorted supply voltage. The DSTATCOM effectively controls the load voltage against variations in the source voltage and in the presence of the harmonic components of the nonlinear load, as shown in Fig. 14. The THD of the load voltage improves to 1.7% and controlled close to 60 V rms.

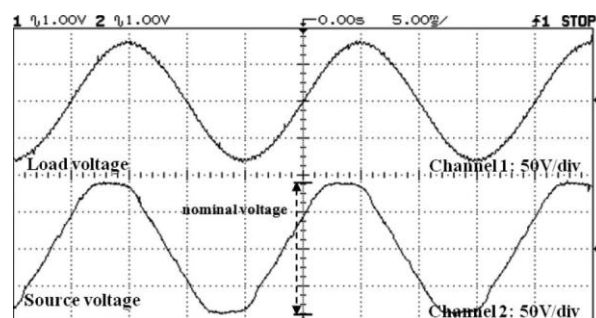


Fig. 13. Load voltage control using DSTATCOM for a non-stiff supply system, showing controlled load voltage and distorted source voltage.

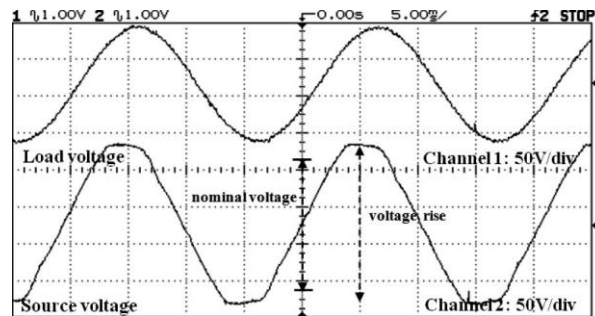


Fig. 14. Load voltage control using DSTATCOM for a non-stiff supply system, showing the controlled load voltage and a voltage rise condition of the source voltage.

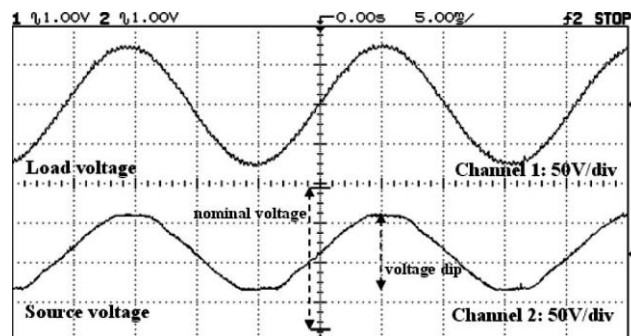


Fig. 15. Load voltage control using the DVR for a stiff supply system, showing controlled load voltage and the voltage dip condition of the source voltage.

Fig. 15 shows the load voltage control using DSTATCOM when the supply undergoes the condition of voltage rise. As predicted in Fig. 9 that the voltage control using DVR for non-stiff source, does not provide attenuation to the high-frequency nonlinear load component.

5.2 Load Voltage Control in Strong AC Supply System

As discussed earlier for the realization of the strong ac system, the ac source is directly connected to the PCC. With this arrangement, the source voltage will directly appear across the load and there is no control of the DSTATCOM over variations in the source voltage. The DVR is useful in this situation. Fig. 15 shows the load voltage control using DVR when the feeder is stiff. The THD of the controlled load voltage is 1.9%. In this case, the DVR control is effective against the variations in the source voltage and harmonics of the nonlinear load. The source voltage again shows the voltage dip condition in Fig. 16.

Fig. 17 shows the load voltage control against sag in the source voltage by the DVR for the stiff supply system. The figure also shows the changing condition of the source voltage.

From the aforementioned experimental results, it is verified that the DSTATCOM is a suitable compensator for the nonlinear load supplied from the non-stiff source. For the other case, the DVR is a suitable compensator when the nonlinear load is supplied from the stiff source.

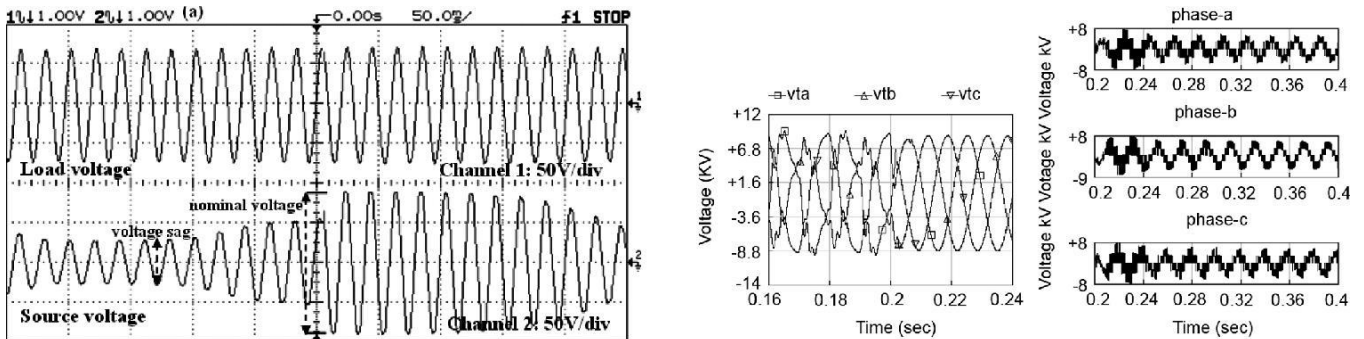


Fig. 16. Load voltage control against sag in the source voltage, using DVR for Fig. 17. (a) Load voltage for three-phase distribution system, DSTATCOM the stiff supply system is connected at 0.2 s. (b) Seven-level inverter output voltages.

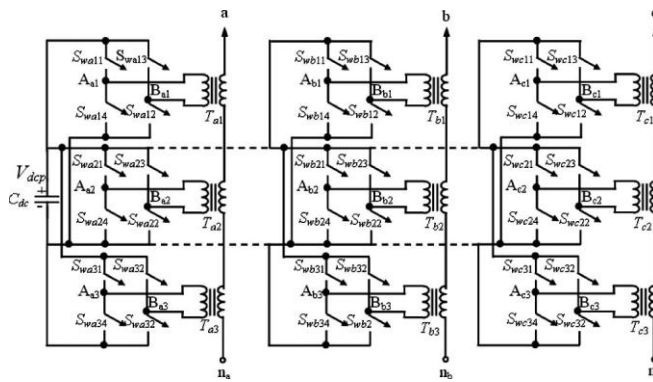


Fig. 18. Three-phase seven-level cascaded transformer H-bridge VSC.

VI SIMULATION STUDIES ON THE THREE-PHASE DISTRIBUTION SYSTEM

In this section, the load voltage of a three-phase four-wire 11-kV distribution system is controlled. The data for the distribution system are given in Table III. The data have the same per unit values as given in Table I.

The converter topology based on the seven-level cascaded transformer multilevel inverter as proposed in [25] and shown in Fig. 18 has been used for the DSTATCOM and the DVR.

The switches $S_{wa11}, S_{wb12}, S_{wc44}$ shown in Fig. 18 represent IGBT with an antiparallel diode. This topology is chosen according to the commonly available IGBT device ratings suitable for the PWM switching scheme [25].

In this topology, a common dc link has been considered for all cells of the three phases of the converter. This dc-link voltage is represented by V_{dc} across the dc-link capacitor C_{dc} . In order to provide the isolation and



voltageboost, the cascading transformers $T_{a1}T_{a2}...T_{c3}$, connected across the H-bridge terminals $A_{a1}B_{a1}A_{a2}B_{a2}...A_{c3}B_{c3}$ are used with each cell of the converter as shown in Fig. 18. For the DSTATCOM, the three terminals a, b, c of the converter are connected to the three phases of the distribution system at the PCC. The other three terminals n_a, n_b , and n_c are joined together and connected to the fourth wire (neutral) of the distribution system. For the DVR, the three terminals a, b, c of the converter, are connected to the three phases at the load bus. The other three terminals n_a, n_b , and n_c are connected to the three phases at the PCC.

VII CONCLUSION

The performance of the VSC-based shunt and series compensators (i.e., DSTATCOM and DVR with the presented topology) has been analyzed in voltage control mode through closed-loop frequency-response characteristics. It is shown that for the weak ac supply system, the load voltage control using DSTATCOM has large bandwidth and good attenuation in source voltage and nonlinear load perturbations. However, the DVR in this case passes high-frequency load components almost unattenuated and causes the presence of notches in the load voltage. For the case of a strong ac supply system, the DVR has good bandwidth and attenuation properties.

The DSTATCOM in this case cannot control the load bus voltage. The proposed analytical results have been verified through the laboratory experimental model. The generalized converter topology based on cascaded multilevel inverter using multi-carrier phase-shifted PWM can be used for the load voltage control of an MV distribution system, following the proposed control algorithm. The results for the three-phase load voltage control have been verified for an 11-kV distribution system, using seven-level cascaded transformer multilevel converter topology, through simulations.

TABLE I
PER UNIT SYSTEM PARAMETERS

LABORATORY MODEL

Parameters	Numerical value (per unit)
Source voltage v_s	1.0
System frequency f_o	50 Hz.
Feeder impedance ($R_s + j\omega_o L_s$)	(0.02 + j0.1)
Input impedance of the nonlinear load ($R_l + j\omega_o L_l$)	(0.01 + j0.05)
Filter capacitor ($1/\omega_o C_f$)	4.0
Interfacing impedance of a compensator ($R_T + j\omega_o L_T$)	(0.01 + j0.1)
Equivalent dc link voltage V_{dc}	2.0

TABLE II
SYSTEM PARAMETERS USED IN THE EXPERIMENTAL

Parameters	Numerical value
Source voltage v_s	60.0 V rms
System frequency f_o	50 Hz.
Feeder impedance L_s, R_s	10.0 mH, 2.0 Ω
Filter capacitor C_f	77.75 μ F
Transformer voltage ratio	115/230 V, $m=2$
Net interfacing impedance L_T, R_T	10.0 mH, 1.0 Ω
Equivalent dc link voltage V_{dc}	200.0 V
Nonlinear load	$R_{ldc} = 25.0 \Omega, C_{ldc} = 220.0 \mu$ F $L_{lac} = 5.0 \text{ mH}, R_{lac} = 1.0 \Omega$

TABLE III
SYSTEM PARAMETERS USED IN THE THREE-PHASE SIMULATION EXAMPLE

Parameters	Numerical value
Base voltage, base power	11.0 kV rms (L-L), 7500.0 kVA
Frequency f_o	50 Hz.
Feeder impedance L_{sk}, R_{sk} where ($k = a, b, c$)	5.13 mH, 0.32 Ω
Cascaded Transformers $T_{i1}, T_{i2}, T_{i3}; i = a, b, c$	2.0 kV/6.0 kV, 300 kVA for each transformer
Net shunt impedance L_{Tk}, R_{Tk}	7.2 mH, 1.02 Ω
Filter capacitor C_{fk}	50.0 μ F
Common dc link voltage	2.2 kV



REFERENCES

- [1] P. R. Sánchez, E. Acha, J. E. O. Calderon, V. Feliu, and A. G. Cerrada, "A versatile control scheme for a dynamic voltage restorer for power-quality improvement," *IEEE Trans. Power Del.*, vol. 24, no. 1, pp. 277–284, Jan. 2009.
- [2] Y. A. R. I. Mohamed and E. F. E. Saadany, "A control method of grid-connected PWM voltage source inverters to mitigate fast voltage disturbances," *IEEE Trans. Power Syst.*, vol. 24, no. 1, pp. 489–491, Feb. 2009.
- [3] P. Samuel, R. Gupta, and D. Chandra, "Grid interface of photovoltaic-micro turbine hybrid based power for voltage support and control using VSI in rural applications," presented at the IEEE Power Eng. Soc. Gen. Meeting, Calgary, AB, Canada, 2009.
- [4] K. Selvajothi and P. A. Janakiraman, "Reduction of voltage harmonics in single phase inverters using composite observers," *IEEE Trans. Power Del.*, vol. 25, no. 2, pp. 1045–1057, Apr. 2010.
- [5] A. Ghosh and G. Ledwich, "Load compensating DSTATCOM in weak AC systems," *IEEE Trans. Power Del.*, vol. 18, no. 4, pp. 1302–1309, Oct. 2003.
- [6] *IEEE Recommended Practices and Requirements for Harmonic Control in Electrical Power Systems*, IEEE Std. 519-1992, Apr. 12, 1993.
- [7] A. Ghosh, "Performance study of two different compensating devices in a custom power park," *Proc. Inst. Elect. Eng., Gen. Transm. Distrib.*, vol. 152, no. 4, pp. 521–528, Jul. 2005.
- [8] M. H. Haque, "Compensation of distribution system voltage sag by DVR and D-STATCOM," in *Proc. IEEE Porto Power Tech Conf.*, Sep. 2001, vol. 1,5, pp. 10–13.
- [9] G. Ledwich and A. Ghosh, "A flexible DSTATCOM operating in voltage or current control mode," *Proc. Inst. Elect. Eng., Gen., Transm. Distrib.*, vol. 149, no. 2, pp. 215–224, Mar. 2002.
- [10] M. K. Mishra, A. Ghosh, and A. Joshi, "Operation of a DSTATCOM in voltage control mode," *IEEE Trans. Power Del.*, vol. 18, no. 1, pp. 258–264, Jan. 2003.
- [11] R. Gupta and A. Ghosh, "Frequency-domain characterization of sliding mode control of an inverter used in DSTATCOM application," *IEEE Trans. Circuits Syst. I, Reg. Papers*, vol. 53, no. 3, pp. 662–676, Mar. 2006.



- [12] B. Singh, A. Adya, A. P. Mittal, J. R. P. Gupta, and B. N. Singh, "Application of DSTATCOM for mitigation of voltage sag for motor loads in isolated distribution systems," in *Proc. IEEE Int. Symp. Ind. Electronics*, Jul. 9–13, 2006, vol. 3, pp. 1806–1811.
- [13] J. Godsk, M. Newman, H. Nielsen, and F. Blaabjerg, "Control and testing of a dynamic voltage restorer (DVR) at medium voltage level," *IEEE Trans. Power Electron.*, vol. 19, no. 3, pp. 806–813, Aug. 2002.
- [14] H. Kim and S. K. Sul, "Compensation voltage control in dynamic voltage restorer by use of feed forward and state feedback scheme," *IEEE Trans. Power Electron.*, vol. 20, no. 5, pp. 1169–1177, Sep. 2005.
- [15] D. M. Vilathgamuwa, H. M. Wijekoon, and S. S. Choi, "A novel technique to compensate voltage sags in multilane distribution system—The interline dynamic voltage restorer," *IEEE Trans. Ind. Electron.*, vol. 53, no. 5, pp. 1603–1611, Oct. 2006.
- [16] Y. W. Li, D. M. Vilathgamuwa, F. Blaabjerg, and P. C. Loh, "A robust control scheme for medium-voltage-level DVR implementation," *IEEE Trans. Ind. Electron.*, vol. 54, no. 4, pp. 2249–2261, Oct. 2006.
- [17] R. Gupta, A. Ghosh, and A. Joshi, "Switching characterization of cas-caded multilevel inverter controlled systems," *IEEE Trans. Ind. Electron.*, vol. 55, no. 3, pp. 1047–1058, Mar. 2008.
- [18] M. J. Newman, D. G. Holmes, J. G. Nielsen, and F. Blaabjerg, "A dynamic voltage restorer (DVR) with selective harmonic compensation at medium voltage level," *IEEE Trans. Ind. Appl.*, vol. 41, no. 6, pp. 1744–1753, Nov./Dec. 2005.
- [19] I. R. Filho, J. L. S. Neto, L. G. Rolim, and M. Aredes, "Design and implementation of a low cost series compensator for voltage sags," in *Proc. IEEE Int. Symp. Ind. Electronics*, Jul. 9–13, 2006, vol. 3, pp. 1353–1357.
- [20] F. A. L. Jowder, "Design and analysis of dynamic voltage restorer for deep voltage sag and harmonic compensation," *Proc. Inst. Eng. Technol. Gen. Transm. Distrib.*, vol. 3, no. 6, pp. 547–560, 2009.
- [21] P. S. Sensarma, K. R. Padiyar, and V. Ramnarayan, "Analysis and performance evaluation of a distribution STATCOM for compensating voltage fluctuations," *IEEE Trans. Power Del.*, vol. 16, no. 2, pp. 259–264, Apr. 2001.
- [22] J. G. Nielsen, F. Blaabjerg, and N. Mohan, "Control strategies for dynamic voltage restorer compensating voltage sags with phase jump," in *Proc. Appl. Power Electr. Conf. Exp.*, Mar. 4–8, 2001, vol. 2, pp. 1267–1273.
- [23] G. Joos, S. Chen, and L. Lopes, "Closed-loop state variable control of dynamic voltage restorers with fast compensation characteristics," in *Proc. IEEE Ind. Appl. Conf.*, Oct. 3–7, 2004, vol. 4, pp. 2252–2258.
- [24] M. A. E. Alali, Y. A. Chapuis, S. Saadate, and F. Braun, "Advanced common control method for shunt and series active compensators used in power quality improvement," *Proc. Inst. Elect. Eng., Elect. Power Appl.*, vol. 151, no. 6, pp. 658–665, Nov. 2006.
- [25] R. Gupta, A. Ghosh, and A. Joshi, "Generalized converter modulation and loss estimation for grid interface applications," in *Proc. IEEE Power Eng. Soc. Gen. Meeting*, Jul. 2008, vol. 6, pp. 20–24.



- [26] H. Patel and V. Agarwal, "Control of a stand-alone inverter-based distributed generation source for voltage regulation and harmonic compensation," *IEEE Trans. Power Del.*, vol. 23, no. 2, pp. 1113–1120, Apr. 2008.
- [27] R. Gupta, A. Ghosh, and A. Joshi, "Cascaded multilevel control of DSTATCOM using multiband hysteresis modulation," in *Proc. IEEE Power Eng. Soc. Gen. Meeting*, Jun. 2006, vol. 7, pp. 18–22.
- [28] F. Z. Peng, "Application issues of active power filters," *IEEE Ind. Appl. Mag.*, vol. 4, no. 5, pp. 21–30, Sep./Oct. 1998.
- [29] J. G. Nielsen and F. Blaabjerg, "A detailed comparison of system topologies for dynamic voltage restorers," *IEEE Trans. Ind. Appl.*, vol. 41, no. 5, pp. 1272–1280, Sep./Oct. 2005.
- [30] K. J. Astrom and B. Wittenmark, *Computer Controlled Systems: Theory and Design*. Englewood Cliffs, NJ: Prentice-Hall, 1984.
- [31] R. Gupta, A. Ghosh, and A. Joshi, "Characteristic analysis for multi-sampled digital implementation of fixed-switching-frequency closed-loop modulation of voltage-source inverter," *IEEE Trans. Ind. Electron.*, vol. 56, no. 7, pp. 2382–2392, Jul. 2009.
- [32] C. S. Lam, M. C. Wong, and Y. D. Han, "Voltage swell and over-voltage compensation with unidirectional power flow controlled dynamic voltage restorer," *IEEE Trans. Power Del.*, vol. 23, no. 4, pp. 2513–2521, Oct. 2006.